Available online at www.sciencedirect.com
SCIENCE DIRECT®
Journal of Organometallic Chemistry 687 (2003) 365–376
Journal of Organometallic Chemistry
www.elsevier.com/locate/jorganchem

Structural and kinetic effects of chloride ions in the palladium-catalyzed allylic substitutions

Thibault Cantat, Emilie Génin, Claire Giroud, Gilbert Meyer, Anny Jutand *

Ecole Normale Supérieure, Département de Chimie, UMR CNRS-ENS-UPMC 8640, 24, Rue Lhomond, F-75231 Paris Cedex 5, France

Received 27 May 2003; received in revised form 27 May 2003; accepted 29 July 2003

Dedicated to Professor Jean-Pierre Genêt on the occasion of his 60th birthday

Abstract

Addition of ligands to $[Pd(\eta^3\text{-RCH–CH–CH}_2)(\mu\text{-Cl})]_2$ or chloride ions to cationic $[(\eta^3\text{-RCH–CH–CH}_2)PdL_2]^+BF_4^-$ induces the formation of neutral complexes η^1-RCH=CH–CH_2–$PdClL_2$ (R = H with L = (4-Cl–C_6H_4)$_3$P, (4-CH_3–C_6H_4)$_3$P, (4-CF_3–C_6H_4)$_3$P or L_2 = 1,2-bis(diphenylphosphino)butane (dppb), 1,1′-bis(diphenylphosphino)ferrocene (dppf); R = Ph with L = (4-Cl–C_6H_4)$_3$P), instead of the expected cationic complexes $[(\eta^3\text{-RCH–CH–CH}_2)PdL_2]^+Cl^-$. In the presence of chloride ions, the reaction of morpholine with the cationic complexes $[(\eta^3\text{-allyl})Pd(PAr_3)_2]^+BF_4^-$ (Ar = 4-Cl–C_6H_4, 4-CH_3–C_6H_4) goes slower and involves both cationic $[(\eta^3\text{-allyl})Pd(PAr_3)_2]^+$ and neutral η^1-allyl-$PdCl(PAr_3)_2$ complexes as reactive species in equilibrium with Cl^-. The cationic complex is more reactive than the neutral one. However, their relative contribution in the reaction strongly depends on the chloride concentration, which controls their relative concentration. The neutral η^1-allyl-$PdCl(PAr_3)_2$ may become the major reactive species at high chloride concentration. Consequently, $[Pd(\eta^3\text{-allyl})(\mu\text{-Cl})]_2$ associated with ligands or cationic $[(\eta^3\text{-allyl})PdL_2]^+BF_4^-$, used indifferently as precursors in palladium-catalyzed allylic substitutions, are not equivalent. In both situations, the mechanism of the Pd-catalyzed allylic substitution depends on the concentration of the chloride ions, delivered by the precursor or purposely added, that determines which species, $[(\eta^3\text{-allyl})PdL_2]^+$ or/and η^1-allyl-$PdClL_2$ are involved in the nucleophilic attack with consequences on the rate of the reaction and probably on its regioselectivity. Consequently, the chloride ions of the catalytic precursors $[Pd(\eta^3\text{-allyl})(\mu\text{-Cl})]_2$ must not be considered as 'innocent' ligands.

Keywords: Allylic substitution; Allyl complex; Chloride ions; Kinetics; Mechanism; Palladium

1. Introduction

Nucleophilic substitutions on allylic acetates are catalyzed by palladium complexes (Tsuji–Trost reactions (Eq. 1) [1].

The catalytic cycle is initiated by a Pd^0L_2 complex (L = PAr_3 or L_2 = P,P; P,N ligands) involved in a reversible oxidative addition which generates a cationic $[(\eta^3\text{-allyl})Pd^{II}L_2]^+$ complexes with AcO^- as the counter anion (Scheme 1) [2].

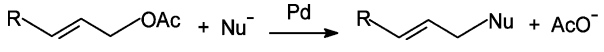

The cationic complex $[(\eta^3\text{-allyl})Pd^{II}L_2]^+$ is supposed to be the key intermediate that reacts with the nucleophile to give the substitution product and the active Pd^0 catalyst [1]. It is why $(\eta^3\text{-allyl})Pd^{II}$ complexes are often used as catalytic precursors of Pd^0 complexes after reaction with the nucleophile. Two kinds of $(\eta^3\text{-allyl})Pd^{II}$ are generally used: (i) dimeric $[Pd^{II}(\eta^3\text{-allyl})(\mu\text{-Cl})]_2$ (**1**) associated with ligands; or (ii) cationic complexes $[(\eta^3\text{-allyl})Pd^{II}L_2]^+$ (**2**$^+$) associated with an innocent counter anion Y^- ($Y^- = BF_4^-$, PF_6^-, TfO^- or TsO^-) [1].

However, in 2001, we established that precursors **1** and **2**$^+$, Y^- were not equivalent [3]. Indeed, complexes **1** (R = H, Ph, Scheme 2) associated with 4 equivalent L (PPh_3), do not generate the cationic complexes **2**$^+$ when the chloride ions have not been quenched by a cation, but give neutral complexes η^1-allyl-$Pd^{II}ClL_2$ (**3**) in

* Corresponding author. Tel.: +33-1-44323872; fax: +33-1-44323325.
E-mail address: anny.jutand@ens.fr (A. Jutand).

0022-328X/03/$ - see front matter © 2003 Elsevier B.V. All rights reserved.
doi:10.1016/S0022-328X(03)00791-5

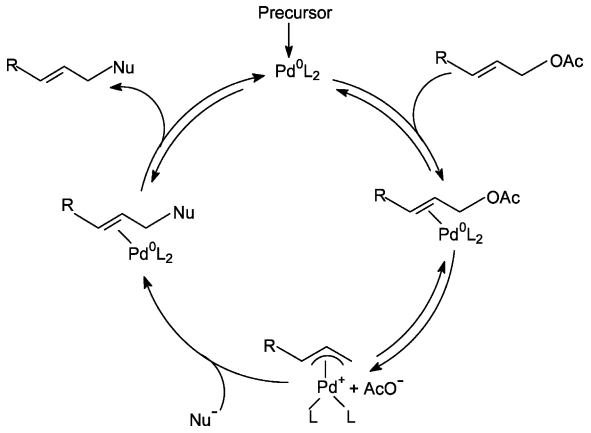

Scheme 1.

dynamic equilibrium (route B in Scheme 2). This reaction with R = H and L = PPh_3 was already reported by Powell and Shaw in 1967 [4].

Moreover, we have established that complexes **3** are always formed in the presence of chloride ions, i.e.: (i) when chloride ions are added to $\mathbf{2}^+, BF_4^-$ (route C in Scheme 2); (ii) when the oxidative addition of allylic acetates to $Pd^0(dba)_2 + 2PPh_3$ is performed in the presence of Cl^- (route D in Scheme 2); or (iii) in the oxidative addition of allylic chlorides to $Pd^0(PPh_3)_4$ (route E in Scheme 2) [3].

Consequently, when the ligand is PPh_3, the postulated cationic complex $[(\eta^3\text{-allyl})Pd(PPh_3)_2]^+X^-$ (X = OAc or Cl) which is supposed to react with the nucleophile is not formed as a major complex in the presence of Cl^- ions which are either delivered by the catalytic precursor or purposely added. The major complexes are neutral η^1-allyl-$PdCl(PPh_3)_2$.

In 2001, Braunstein et al. reported the characterization of a η^1-allyl-$Pd^{II}Cl$(P,N) complex (P,N = bis(oxazoline)phenylphosphonite) [5]. In 2002, Kollmar and Helmchen reported the synthesis of a η^1-allyl-PdCl(P,N) (P,N = phosphinooxazoline) complex [6]. In both cases, the η^1-allyl-PdCl complexes were obtained by treating a dimer $[Pd(\eta^3\text{-allyl})(\mu\text{-Cl})]_2$ with 2 equivalent of the corresponding P,N ligand, in the absence of any chloride scavenger. On the other hand, the decomposition of $(\eta^3$-allyl)Pd^{II} complexes may be induced by the addition of chloride ions [7].

In 1981, Akermark et al. reported a difference of reactivity of dimethylamine with an isolated cationic complex $[(\eta^3\text{-}CH_3\text{–}CH\text{–}CH\text{–}CH_2)Pd(PPh_3)_2]^+BF_4^-$, when compared to the neutral complex $\eta^1\text{-}CH_3\text{–}CH{=}CH\text{–}CH_2\text{–}PdCl(PPh_3)_2$, supposedly generated in situ by reaction of $[Pd^{II}(\eta^3\text{-}CH_3\text{–}CH\text{–}CH\text{–}CH_2)(\mu\text{-Cl})]_2$ with 4 equivalent PPh_3. The regioselectivity of the reaction was also different [8].

When considering palladium-catalyzed allylic substitutions, the efficiency, regioselectivity and enantioselectivity may be affected by the catalytic precursor or by the presence of chloride ions purposely added, as evidenced by Bäckvall [9], Hayashi [10], Lloyd-Jones [11], and Trost's groups [12].

This incited us to investigate the role of chloride ions in the possible formation of neutral η^1-allyl-$Pd^{II}ClL_2$ complexes for different mono- ($L = PAr_3$) or bidentate bisphosphines (L_2 = P,P) and their contribution in the mechanism and kinetics of the nucleophilic attack of morpholine.

2. Results and discussion

2.1. Effect of chloride ions on the structure of (allylic)Pd^{II} complexes: η^3-allyl versus η^1-allyl coordination

2.1.1. Formation of neutral η^1-allyl-$PdClL_2$ (L = monodentate ligand: $(4\text{-}Z\text{–}C_6H_4)_3P$, Z = Cl, CH_3, CF_3)

The two routes B and C in Scheme 2 were explored for the synthesis of (allyl)Pd^{II} complexes in the presence of chloride ions. Even if the monophosphine ligands $(4\text{-}Z\text{–}C_6H_4)_3P$ (Z = Cl, CH_3, CF_3) are not widely used as

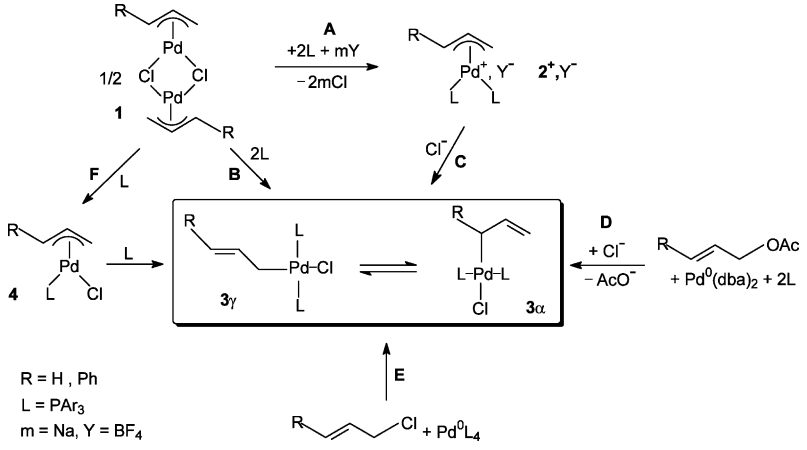

Scheme 2.

palladium ligands in catalytic Tsuji–Trost reactions [1], it was of academic interest to investigate their electronic effect in the formation of neutral η^1-allyl-$Pd^{II}ClL_2$ (**3**). Indeed, the positive charge on the cationic complexes $[(\eta^3\text{-allyl})Pd^{II}L_2]^+$ ($\mathbf{2}^+$) is affected by the electronic properties of the phosphine, with some expected consequences on their reactivity with nucleophiles, including chloride ions.

As for PPh_3, addition of 4 equivalent $(4\text{-}Z\text{–}C_6H_4)_3P$ (Z = Cl, CH_3, CF_3) to the dimer $[Pd(\eta^3\text{-}CH_2\text{–}CH\text{–}CH_2)(\mu\text{-}Cl)]_2$ (**1**) in acetone or chloroform (route B of Scheme 2) resulted in the complete disappearance of the dimer with formation of the neutral complexes η^1-CH_2=CH–CH_2–$PdCl\{(4\text{-}Z\text{–}C_6H_4)_3P\}_2$ (**3a**, Z = Cl; **3b**, Z = CH_3; and **3c**, Z = CF_3, respectively). This is evidenced by the presence in their ^{1}H-NMR spectrum performed in chloroform or acetone of only *two* sets of signals for the protons of the allyl group (Fig. 1a) (instead of the *three* sets of signals observed for the corresponding cationic complexes $[(\eta^3\text{-}CH_2\text{–}CH\text{–}CH_2)Pd\{(4\text{-}Z\text{–}C_6H_4)_3P\}_2]^+BF_4^-$ ($\mathbf{2a}^+$, Z = Cl; $\mathbf{2b}^+$, Z = CH_3; and $\mathbf{2c}^+$, Z = CF_3) in Fig. 1b): (i) one well defined quintet at low field integrating for one H; and (ii) one doublet that may be broad, located at upper field and integrating for 4H (Fig. 1a). The former characterizes the central H of the ligand η^1-CH_2=C*H*–CH_2 whereas the latter characterizes the four terminal H of the ligand η^1-CH_2=CH–CH_2 which become magnetically equivalent due to a fast dynamic

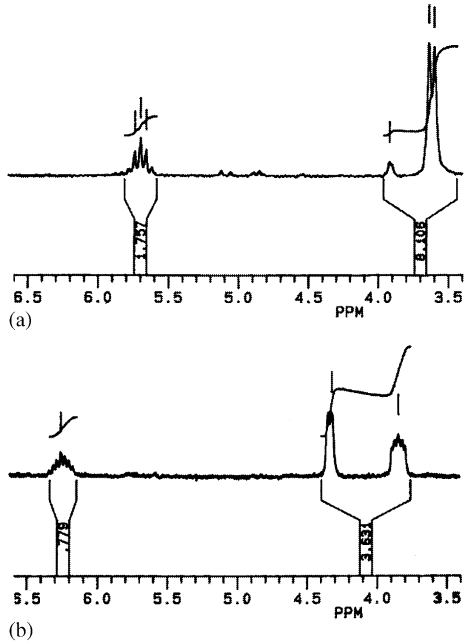

Fig. 1. ^{1}H-NMR spectroscopy performed in acetone-d_6 (250 MHz, TMS). Protons of the allyl ligand of: (a) η^1-CH_2=CH–CH_2–$PdCl\{(4\text{-}Cl\text{–}C_6H_4)_3P\}_2$ (**3a**); (b) $[(\eta^3\text{-}CH_2\text{–}CH\text{–}CH_2)Pd\{(4\text{-}Cl\text{–}C_6H_4)_3P\}_2]^+BF_4^-$ ($\mathbf{2a}^+$, BF_4^-).

equilibrium between two η^1-coordination modes **3α** and **3γ** (Scheme 2) [3,4].

The protons of the allyl ligand of η^1-CH_2=CH–CH_2–$PdCl\{(4\text{-}Z\text{–}C_6H_4)_3P\}_2$ are globally located at upper field than those of the corresponding cationic complexes $[(\eta^3\text{-}CH_2\text{–}CH\text{–}CH_2)Pd\{(4\text{-}Z\text{–}C_6H_4)_3P\}_2]^+$ (compare Fig. 1a and b). Indeed, the ^{1}H-NMR signals of the central H of η^1-CH_2=C*H*–CH_2–$PdCl\{(4\text{-}Z\text{–}C_6H_4)_3P\}_2$ (Z = Cl, CH_3, CF_3, H) are all located at upper field than the central H of the cationic $[(\eta^3\text{-}CH_2\text{–}CH\text{–}CH_2)Pd\{(4\text{-}Z\text{–}C_6H_4)_3P\}_2]^+$ (Z = Cl, CH_3, CF_3, H). Similarly, the signal of the four magnetically equivalent terminal H of η^1-CH_2=CH–CH_2–$PdCl\{(4\text{-}Z\text{–}C_6H_4)_3P\}_2$ are located at upper field than the anti-H of the cationic $[(\eta^3\text{-}CH_2\text{–}CH\text{–}CH_2)Pd\{(4\text{-}Z\text{–}C_6H_4)_3P\}_2]^+$ (Z = Cl, CF_3) (itself always located at higher field than the syn-H) or very close to the anti-H of the cationic $[(\eta^3\text{-}CH_2\text{–}CH\text{–}CH_2)Pd\{(4\text{-}Z\text{–}C_6H_4)_3P\}_2]^+$ (Z = CH_3, H). This shift towards upper field is indicative of the coordination of the chloride to the Pd^{II} center. This implicates a η^1-CH_2=CH–CH_2– coordination to a $Pd^{II}L_2$ moieties because no free phosphine was detected in the ^{31}P-NMR spectra [13]. Traces of the phosphonium salt $[(4\text{-}Z\text{–}C_6H_4)_3P\text{–}CH_2\text{–}CH{=}CH_2]^+$ were also observed in the ^{1}H-NMR spectrum of **3a**–**c**, as when PPh_3 was considered [3,14].

It was also observed by ^{1}H-NMR spectroscopy that addition of 1 equivalent Cl^- (introduced as nBu$_4$NCl) to a solution of the cationic complex $[(\eta^3\text{-}CH_2\text{–}CH\text{–}CH_2)Pd\{(4\text{-}Cl\text{–}C_6H_4)_3P\}_2]^+$ ($\mathbf{2a}^+$,BF_4^-), 17 mM in chloroform, led to the neutral complex η^1-CH_2=CH–CH_2–$PdCl\{(4\text{-}Cl\text{–}C_6H_4)_3P\}_2$ (**3a**) (route C in Scheme 2).

To confirm the formation of the neutral complexes η^1-CH_2=CH–CH_2–$PdCl(PAr_3)_2$ instead of the cationic ones $[(\eta^3\text{-}CH_2\text{–}CH\text{–}CH_2\text{–}Pd(PAr_3)_2]^+Cl^-$, conductivity measurements were performed in DMF in which free ions are usually generated [15]. A solution of the isolated complex η^1-CH_2=CH–CH_2–$PdCl\{(4\text{-}Cl\text{–}C_6H_4)_3P\}_2$ (**3a**), 2 mM in DMF, exhibited a low conductivity of 7 μs cm^{-1} at 25 °C. By comparison the conductivity of the cationic complex $[(\eta^3\text{-}CH_2\text{–}CH\text{–}CH_2)Pd\{(4\text{-}Z\text{–}C_6H_4)_3P\}_2]^+BF_4^-$ ($\mathbf{2a}^+$, BF_4^-), under the same conditions, was 69 μs cm^{-1}. This allows the calculation of the theoretical conductivity of the putative $[(\eta^3\text{-}CH_2\text{–}CH\text{–}CH_2)Pd\{(4\text{-}Cl\text{–}C_6H_4)_3P\}_2]^+Cl^-$ to be close to 64 μs cm^{-1} [16]. Consequently, one can assume that a neutral complex η^1-CH_2=CH–CH_2–$PdCl\{(4\text{-}Cl\text{–}C_6H_4)_3P\}_2$ (**3a**) is indeed generated in the presence of chloride ions (routes B and C of Scheme 2).

Similarly, when 4 equivalent $(4\text{-}Cl\text{–}C_6H_4)_3P$ were added to the dimer $[Pd(\eta^3\text{-}Ph\text{–}CH\text{–}CH\text{–}CH_2)(\mu\text{-}Cl)]_2$ (**1′**) in the absence of a chloride scavenger (route B in Scheme 2), the neutral complex η^1-Ph–CH=CH–CH_2–$PdCl\{(4\text{-}Cl\text{-}\text{–}C_6H_4)_3P\}_2$ (**3a′**) was

generated, as well as when 1 equivalent Cl^- was added to a solution of the cationic complex [(η^3-Ph–CH–CH–CH_2) Pd {(4-Cl–C_6H_4)$_3$P}$_2$]$^+$ BF_4^- (**2a′**$^+$,BF_4^-) in chloroform (route C in Scheme 2). In both cases, **1′** and **2a′**$^+$,BF_4^- were totally converted. As in the allyl series, the ^{1}H-NMR signals of the protons of the allyl ligand of η^1-Ph–CH=CH–CH_2–PdCl{(4-Cl–C_6H_4)$_3$P}$_2$ (**3a′**) were located at higher field (Fig. 2a) than those of the cationic complex [(η^3-Ph–CH–CH–CH_2) Pd {(4-Cl–C_6H_4)$_3$P}$_2$]$^+$ BF_4^- (**2a′**$^+$,BF_4^-) (Fig. 2b).

Whereas in the cinnamyl chloride (*E*)-PhCH=CH–CH_2Cl, the signal of the proton PhC*H* was located at lower field (6.63 ppm) than that of the central PhCH=C*H* (6.30 ppm), the situation was reversed in the complex η^1-Ph–CH=CH–CH_2–PdCl{(4-Cl–C_6H_4)$_3$P}$_2$ (Fig. 2a). This suggests that the PhC*H* proton in the latter neutral complex was shifted to upper field because of a Pd^{II} coordination, as in η^1-Ph–CH(PdClL$_2$)–CH=CH_2, and the involvement of a fast dynamic equilibrium between two η^1 coordination of the cinnamyl ligand (**3γ** and **3α** in Scheme 2, R = H). This was confirmed by the fact that, in the neutral complex, the J_{HH} coupling between PhC*H* and the central H was 13 Hz, an average value that is lower than a trans J_{HH} coupling (e.g. 15.5 Hz in (*E*)-PhC*H*=C*H*–CH_2Cl) but higher than the J_{HH} coupling between an allylic and a vinylic proton (e.g. 7 Hz in PhCH=C*H*–CH_2Cl). Moreover, the allylic CH_2 protons of the neutral complex (3.15 ppm in Fig. 2a) became magnetically equivalent when compared to the two differentiated anti-H and syn-H of the cationic complex (Fig. 2b). Their J_{HH} coupling with the central H was 9 Hz, which is higher than the J_{HH} coupling between an allylic and a vinylic proton (e.g. 7 Hz in PhCH=C*H*–CH_2Cl) due to the contribution of the **3γ** structure. Consequently, the dynamic equilibrium between **3γ** and **3α** observed in the allyl series also operates in the cinnamyl series (Scheme 2, R = Ph) and the observed ^{1}H-NMR spectrum assigned to (**3a′**) is in fact an average spectrum due to a fast dynamic equilibrium between **3γ** and **3α** (Scheme 2, R = H).

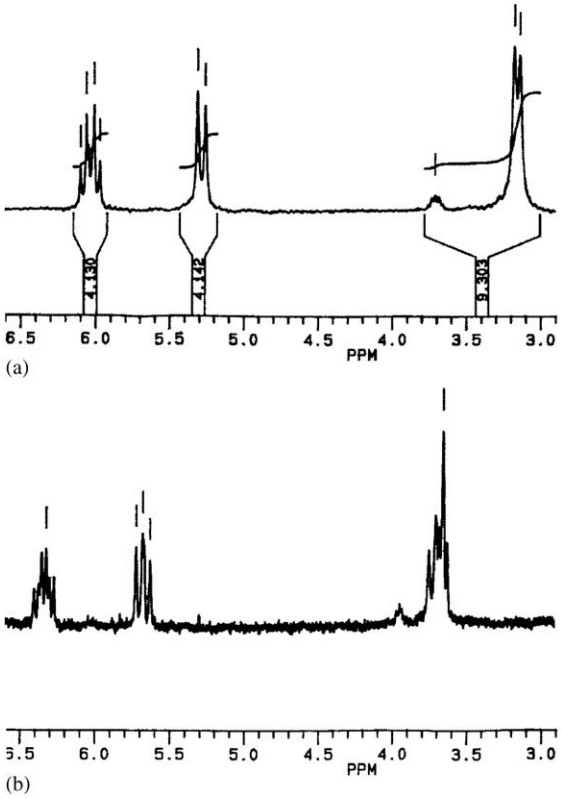

Fig. 2. ^{1}H-NMR spectroscopy performed in $CDCl_3$ (250 MHz, TMS). Protons of the allyl ligand of: (a) η^1-PhCH=CH–CH_2–PdCl{(4-Cl–C_6H_4)$_3$P}$_2$ (**3a′**); (b) [(η^3-PhCH–CH–CH_2)Pd{(4-Cl–C_6H_4)$_3$P}$_2$]$^+$ BF_4^- (**2a′**$^+$, BF_4^-).

This was ultimately confirmed by the fact that the cationic complex (**2a′**$^+$,BF_4^-) was characterized in ^{31}P-NMR spectroscopy by two doublets due to non equivalent phosphine ligands whereas the complex generated in the presence of chloride ions exhibited only one singlet attesting for 2 equivalent ligands sitting in a trans position in the neutral complexes **3γ** and **3α** (Scheme 2, R = Ph). Although J_{PH} couplings were observed for the protons of the allyl ligand of the cationic (η^3-allyl)Pd^{II} complexes (Fig. 2b), no J_{PH} coupling was detectable in the η^1-allyl-Pd^{II} chloride complexes (Fig. 2a). This suggests that either the dynamic equilibrium between **3γ** and **3α** occurs via the dissociation of the phosphine ligand or that the J_{PH} coupling is too small to be detected at 250 MHz because of the cis coordination of the phosphine and the cinnamyl group. As observed in Fig. 2a, the phosphonium salt [cinnamyl-P(4-Cl-C_6H_4)$_3$]$^+$ was not formed in appreciable amount in contrast with [cinnamyl-PPh_3]$^+$ [3,14].

2.1.2. Formation of neutral η^1-allyl-PdCl(P,P) (P,P = bidentate ligand: dppb, dppf)

The route B in Scheme 3 was explored for the synthesis of (allyl)Pd^{II} complexes ligated by bisphosphines, in the presence of chloride ions.

The complexes η^1-CH_2=CH-CH_2-PdCl(dppb) (**5d**) and η^1-CH_2=CH–CH_2–PdCl(dppf) (**5e**) were synthesized by addition of respectively 2 equivalent 1,2-bis(diphenylphosphino)butane (dppb) or 1,1′-bis(diphenylphosphino)ferrocene (dppf) to the dimer [Pd(η^3-CH_2–CH–CH_2)(μ-Cl)]$_2$ (**1**). As in the monodentate series, the ^{1}H-NMR spectrum performed in $CDCl_3$ or acetone-d_6 exhibited only two sets of signals for the allylic protons: (i) one well defined quintet at low field integrating for one H, the central H of the ligand η^1-CH_2=C*H*–CH_2; and (ii) one broad multiplet, located at higher field and integrating for 4H which characterizes the four terminal H of η^1-CH_2=CH–CH_2 that became

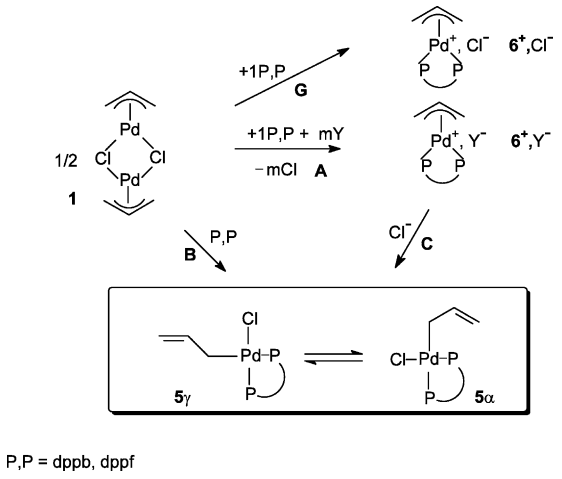

Scheme 3.

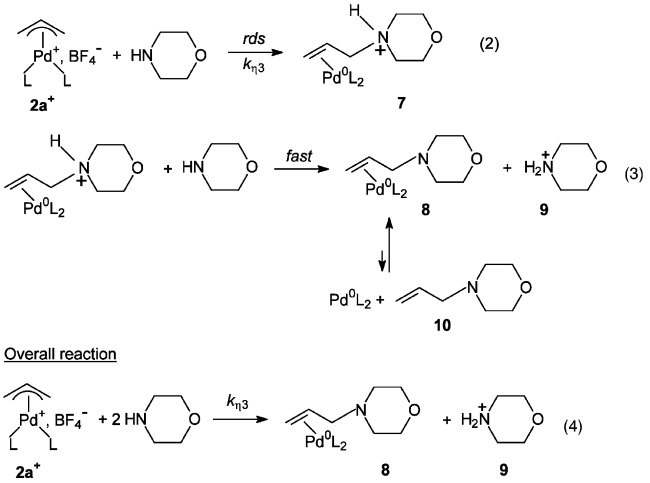

Scheme 4.

magnetically equivalent due to a fast dynamic equilibrium (**5γ** and **5α** in Scheme 3).

A solution of η^1-CH_2=CH–CH_2–PdCl(dppb) (**5d**), 2 mM in DMF, exhibited a low conductivity of 12 μs cm^{-1} [18]. The theoretical conductivity of the putative $[(\eta^3\text{-}CH_2\text{–}CH\text{–}CH_2)Pd(dppb)]^+Cl^-$, 2 mM in DMF, that could have been formed (route G in Scheme 3), was estimated from the known conductivity of $[(\eta^3\text{-}CH_2\text{–}CH\text{–}CH_2)Pd(dppb)]^+AcO^-$ [2a] and found to be close to 124 μs cm^{-1} [19]. Consequently, one can assume that a neutral complex η^1-CH_2=CH–CH_2–PdCl(dppb) (**3d**), is indeed generated in the presence of chloride ions (route B in Scheme 3) instead of the cationic complex, even in a dissociative solvent as DMF [15]. This was ultimately checked by running a ^{1}H-NMR spectrum in DMF-d_7 which exhibited the quintet and the doublet as unique signals characteristic of the neutral complex η^1-CH_2=CH–CH_2–PdCl(dppb), as observed in chloroform and acetone (vide supra).

2.2. Effect of chloride ions on the kinetics of the nucleophilic attack on allylic-Pd^{II} complexes

Cationic complexes $[(\eta^3\text{-allyl})PdL_2]^+$ [20] are postulated to be the reactive species in the nucleophilic attack (Scheme 1) [1]. As evidenced above, cationic complexes $[(\eta^3\text{-allyl})PdL_2]^+BF_4^-$ (L = PAr_3) are easily transformed to the neutral complexes η^1-allyl-$PdClL_2$ in the presence of chloride ions. Consequently, it was of interest to investigate the effect of chloride ions on the kinetics of the nucleophilic reaction.

2.2.1. Kinetics of the reaction of morpholine with the cationic complexes $[(\eta^3\text{-}CH_2\text{–}CH\text{–}CH_2)PdL_2]^+BF_4^-$ ($L = (4\text{-}Cl\text{–}C_6H_4)_3P$, $(4\text{-}CH_3\text{–}C_6H_4)_3P$) in the absence of chloride ions

Morpholine was chosen as nucleophile. Its reaction with $[(\eta^3\text{-}CH_2\text{–}CH\text{–}CH_2)Pd\{(4\text{-}Cl\text{–}C_6H_4)_3P\}_2]^+BF_4^-$ ($\mathbf{2a}^+, BF_4^-$), performed in DMF at room temperature, produced the substitution product **10** (Scheme 4), identified by ^{1}H-NMR spectroscopy [21]. In a first approach, the simple nonsubstituted allyl complex was investigated to by-pass regioselectivity problems.

The reaction was first monitored by cyclic voltammetry. The complex $\mathbf{2a}^+, BF_4^-$ (2 mM) in DMF (containing $n\text{Bu}_4\text{NBF}_4$, 0.3 M) exhibited a reduction peak R_1 at $E^p_{R_1} = -1.39$ V versus SCE and no oxidation peak. After addition of 20 equivalent morpholine, a new reduction peak R_2 appeared at less negative potential: $E^p_{R_2} = -1.02$ V, while the reduction peak R_1 of $\mathbf{2a}^+, BF_4^-$ was no longer observed. When the potential was scanned to oxidation first, an oxidation peak O_3 was detected at $E^p_{O_3} = +0.25$ V. From these voltammograms, one concludes that the morpholine reacts with $\mathbf{2a}^+, BF_4^-$ (its reduction peak R_1, whose reduction peak current is proportional to its concentration, was no longer detected) to generate a Pd^0 complex characterized by its oxidation peak O_3. This reaction also generates a species, which is reduced at R_2. The latter was identified as the protonated morpholine **9** (Scheme 4). The presence of **9** more easily reduced than $\mathbf{2a}^+, BF_4^-$ did not allow the investigation of the kinetics of the reaction of $\mathbf{2a}^+, BF_4^-$ with morpholine, by monitoring the decay of its reduction peak current versus time. Moreover, the reaction was too fast at 25 °C to be monitored by cyclic voltammetry [22].

The kinetics of the nucleophilic attack was thus investigated by UV spectroscopy as reported by Kuhn and Mayr for the cationic complex $[(\eta^3\text{-Ph–CH–CH–}CH_2)Pd(PPh_3)_2]^+BF_4^-$ in dichloromethane [23]. In that case, the decay of the absorbance of $[(\eta^3\text{-Ph–CH–CH–}CH_2)Pd(PPh_3)_2]^+BF_4^-$ in the presence of morpholine was monitored versus time. However, since the complex $[(\eta^3\text{-Ph–CH–CH–}CH_2)Pd\{(4\text{-Cl–}C_6H_4)_3P\}_2]^+BF_4^-$ ($\mathbf{2a}^+, BF_4^-$) did not exhibit any absorbance in the range

300–800 nm, another strategy was chosen. After addition of 10 equivalent morpholine to $\mathbf{2a}^+, BF_4^-$ (0.5 mM) in DMF at 25 °C, an absorption band appeared at 323 nm (absorbance $D = 0.34$) which characterizes the Pd^0 complex **8** (Scheme 4), as attested by the UV spectroscopy performed on a solution of $Pd^0\{(4\text{-Cl}–C_6H_4)_3P\}_4$ and the substitution product **10**.

When less than 2 equivalent morpholine was added to $\mathbf{2a}^+, BF_4^-$ (0.5 mM) in DMF, the absorbance of the Pd^0 complex **8** was less than 0.34. One additional equivalent morpholine was required to observe the absorbance of 0.34 obtained when a large excess morpholine was used. Addition of more morpholine did not affect the final absorbance. This shows that the complete substitution on $\mathbf{2a}^+$ (Eq. 4 in Scheme 4) requires 2 equivalent morpholine. The deprotonation involved in a second step (Eq. 3 in Scheme 4) is thus faster than the nucleophilic reaction (Eq. 2 in Scheme 4). Consequently, the rate of formation of the Pd^0 complex **8** (Eq. 4) which could easily be monitored by UV spectroscopy, is indicative of the rate of the nucleophilic attack (Eq. 2).

In order to anticipate any effect of the ionic strength that might occur when the nucleophilic attack of morpholine will be investigated in the presence of Cl^- introduced as $n\text{Bu}_4\text{NCl}$ (free ions in DMF, vide supra), the kinetics of reaction (4) was investigated in the absence and presence of $n\text{Bu}_4\text{NBF}_4$ (0.3 M), i.e. at low and high ionic strength. To observe reasonable reaction times, the kinetics of the reaction in Eq. 4 (rate constant: $k_{\eta 3}$) was performed at −25 °C. Fig. 3a exhibits the absorbance of the Pd^0 complex **8**, generated after addition of 10 equivalent morpholine to $\mathbf{2a}^+, BF_4^-$ (0.5 mM) in DMF, versus time.

According to the mechanism postulated in Scheme 4, the kinetic law of reaction (4) is given in given in Eq. (5) (M: morpholine).

$$d[\mathbf{2a}^+]/dt = -d[\mathbf{8}]/dt = -k_{\eta 3}[\mathbf{2a}^+][M] \quad (5)$$

In the presence of excess morpholine (pseudo first order conditions), the integration of Eq. (5) gives Eq. (6) ($x = ([\mathbf{8}]_{lim} - [\mathbf{8}])/[\mathbf{8}]_{lim} = (D_{lim} - D)/D_{lim}$ with D: absorbance of **8** at t and D_{lim}: final absorbance of **8**).

$$\ln x = -k_{\eta 3}[M]t = -k_{exp}t \quad (6)$$

The plot of $\ln x$ versus time was linear (Fig. 3b): $\ln x = -k_{exp}t$. Plotting k_{exp} versus morpholine concentration afforded a straight line (Fig. 3c), which confirms that the reaction order in morpholine is one in agreement with the mechanism of Scheme 4: $k_{exp} = k_{\eta 3}[M]$. This reaction order was also found by Kuhn and Mayr for the related complex $[(\eta^3\text{-Ph–CH–CH–CH}_2)\text{Pd}(\text{PPh}_3)_2]^+ BF_4^-$ in dichloromethane [23].

The value of $k_{\eta 3}$ was then calculated from the slope of the straight line in Fig. 3c: $k_{\eta 3} = 5.6\ M^{-1}\ s^{-1}$ (DMF, −25 °C, $n\text{Bu}_4\text{NBF}_4$, 0.3 M). The rate constant was also

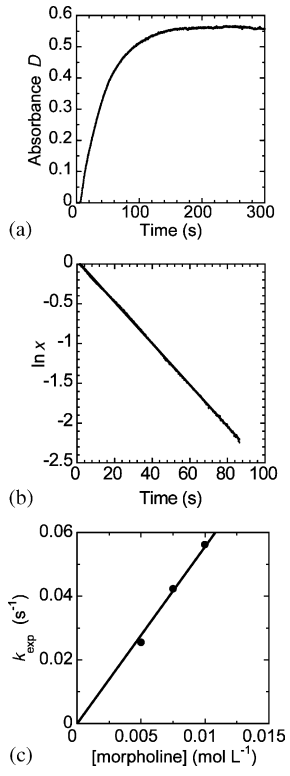

Fig. 3. Kinetics of the reaction of morpholine with the cationic complex $[(\eta^3\text{-CH}_2\text{–CH–CH}_2)\text{Pd}(\text{PAr}_3)_2]^+ BF_4^-$ (Ar = 4-Cl–C_6H_4) ($\mathbf{2a}^+, BF_4^-$) (0.5 mM) in DMF containing $n\text{Bu}_4\text{NBF}_4$ (0.3 M) at −25 °C, monitored by UV spectroscopy. (a) Absorbance at 323 mm of the Pd^0 complex **8** versus time, after addition of 10 equivalent morpholine; (b) variation of ln x versus time ($x = ([\mathbf{8}]_{lim} - [\mathbf{8}])/[\mathbf{8}]_{lim} = (D_{lim} - D)/D_{lim}$ with D: absorbance of **8** at t and D_{lim}: final absorbance of **8** determined in Fig. 1a). $\ln x = -k_{exp}t$; (c) reaction order in morpholine: plot of k_{exp} versus the morpholine concentration. $k_{exp} = k_{\eta 3}$[morpholine].

determined in the absence of $n\text{Bu}_4\text{NBF}_4$: $k_{\eta 3} = 4.2\ M^{-1}\ s^{-1}$ (DMF, −25 °C). Comparison of the two values indicates that the effect of the increasing ionic strength on the rate of the nucleophilic attack of morpholine on the cationic complex $\mathbf{2a}^+$ was relatively low (accelerating effect of 30%) despite the fact that a cationic Pd^{II} complex was involved in the reaction.

The reaction of morpholine (2 mM) with the cationic complex $[(\eta^3\text{-CH}_2\text{–CH–CH}_2)\text{Pd}\{(4\text{-Me–C}_6\text{H}_4)_3\text{P}\}_2]^+ BF_4^-$ ($\mathbf{2b}^+, BF_4^-$) (1 mM) was investigated at 25 °C by UV spectroscopy in the absence of $n\text{Bu}_4\text{NBF}_4$ [24]. The reaction was found to be slower than that with $\mathbf{2a}^+, BF_4^-$, with a rate constant of $k_{\eta 3} = 1\ M^{-1}\ s^{-1}$ (DMF, 25 °C) (Fig. 4, Table 1) [25]. This is consistent with the fact that the ligand $(4\text{-Me-C}_6\text{H}_4)_3\text{P}$ of the cationic Pd^{II} center is more electron rich than $(4\text{-Cl–C}_6\text{H}_4)_3\text{P}$, which disfavors the external nucleophilic attack on the allyl ligand [1].

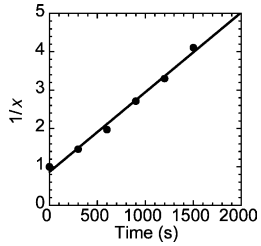

Fig. 4. Kinetics of the reaction of morpholine (2 mM) with the cationic complex $[(\eta^3\text{-}CH_2\text{–}CH\text{–}CH_2)Pd(PAr_3)_2]^+BF_4^-$ (Ar = 4-Me-C_6H_4) (**2b**$^+$, BF_4^-) ($C_0 = 1$ mM) in DMF at 25 °C, monitored by UV spectroscopy at 296 mm. Variation of $1/x$ versus time ($x = ([\mathbf{8}]_{lim} - [\mathbf{8}])/[\mathbf{8}]_{lim} = (D_{lim} - D)/D_{lim}$ with D: absorbance of **8** at t and D_{lim}: final absorbance of **8**. $1/x = 2k_{\eta 3}C_0t + 1$ [25].

Table 1
Comparative intrinsic reactivity of cationic $[(\eta^3\text{-allyl})PdL_2]^+$ and neutral η^1-allyl-$PdClL_2$ complexes with morpholine in DMF at 25 °C (Scheme 5)

L = (4-Z–C_6H_4)$_3$P	$k_{\eta 1}$ ($M^{-1}\,s^{-1}$)	$k_{\eta 3}$ ($M^{-1}\,s^{-1}$)	K_{Cl} (M^{-1})
Z = Cl	0.91	94	58×10^3
Z = Me	0.29	1	2.4×10^3

2.2.2. Kinetics of the reaction of morpholine with the cationic complexes $[(\eta^3\text{-}CH_2\text{–}CH\text{–}CH_2)PdL_2]^+BF_4^-$ ($L = (4\text{-}Cl\text{–}C_6H_4)_3P$); ($(4\text{-}CH_3\text{–}C_6H_4)_3P$)) in presence of chloride ions

The effect of chloride ions on the reactivity of **2a**$^+$, BF_4^- ($C_0 = 0.5$ mM) with morpholine was investigated in DMF by UV spectroscopy, by monitoring the formation of the Pd^0 complex **8** versus time. The chloride ions were introduced as nBu$_4$NCl, in the concentration range of 4.9–8.8 mM to minimize any effect of the variation of the ionic strength (vide supra). The nucleophilic attack went slower and slower when the Cl^- concentration was increased. This cannot be interpreted as a consequence of the increasing ionic strength, since the effect of the ionic strength was to slightly accelerate the nucleophilic attack (vide supra). A specific effect of nBu$_4$NCl must thus be considered.

As established in Section 2.1.1, the addition of Cl^- as nBu$_4$NCl to the cationic complex $[(\eta^3\text{-}CH_2\text{–}CH\text{–}CH_2)Pd\{(4\text{-}Cl\text{–}C_6H_4)_3P\}_2]^+BF_4^-$ (**2a**$^+$, BF_4^-) induced the formation of the neutral complex η^1-CH_2=CH–CH_2–PdCl{(4-Cl–C_6H_4)$_3$P)}$_2$ (**3a**). It was checked by ^{1}H-NMR spectroscopy in chloroform that reaction of the isolated neutral complex **3a** with morpholine gave the substitution product **10**. However, the fact that the rate of the nucleophilic attack on the cationic complex **2a**$^+$, BF_4^- depends on the Cl^- concentration suggests that the two complexes **2a**$^+$ and **3a** are in equilibrium with the Cl^- (Scheme 5) with $K_{Cl}[Cl^-] \gg 1$, because the cationic complex **2a**$^+$ was no longer detected in the presence of 1 equivalent Cl^-

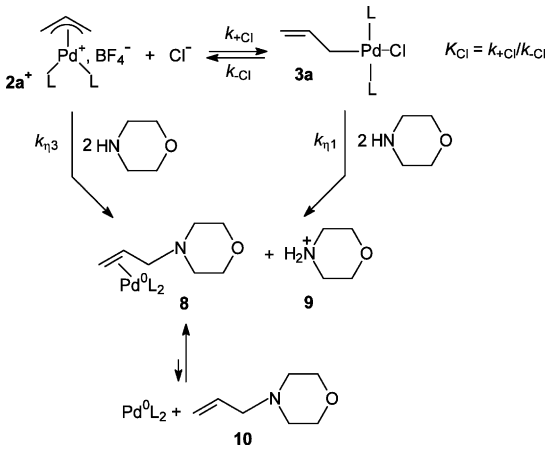

Scheme 5.

($C_0 = 0.5$ mM). It was of interest to determine whether the cationic complex **2a**$^+$ remained the reactive complex even in the presence of a large excess of Cl^- or whether both complexes **2a**$^+$ and **3a** react in parallel with morpholine to give the same substitution product **10** (Scheme 5). The reaction of morpholine with **2a**$^+$ is known to be an external attack onto the η^3-allyl ligand [1] whereas reaction of morpholine with **3a** would be an attack of the η^1-allyl ligand by a S_N2' substitution, as proposed by Akermark et al. [8,26].

According to Scheme 5, the kinetic law is given in Eq. (7) (M: morpholine).

$$d[\mathbf{8}]/dt = k_{\eta 3}[\mathbf{2a}^+][M] + k_{\eta 1}[\mathbf{3a}][M] \quad (7)$$

Eq. (8) is obtained upon considering steady state approximation for complex **2a**$^+$.

$$\frac{d[\mathbf{8}]}{dt} = [\mathbf{3a}][M]\left(k_{\eta 1} + \frac{k_{\eta 3}k_{-Cl}}{k_{+Cl}[Cl^-] + k_{\eta 3}[M]}\right) \quad (8)$$

It simplifies into Eq. (9) when considering that $k_{+Cl}[Cl^-] \gg k_{\eta 3}[M]$.

$$\frac{d[\mathbf{8}]}{dt} = [\mathbf{3a}][M]\left(k_{\eta 1} + \frac{k_{\eta 3}k_{-Cl}}{k_{+Cl}[Cl^-]}\right) = [\mathbf{3a}][M]\left(k_{\eta 1} + \frac{k_{\eta 3}}{K_{Cl}[Cl^-]}\right) \quad (9)$$

The integration of Eq. (9) gives Eq. (10) (when $[Cl^-] > 10C_0$) with an apparent rate constant k_{app} expressed in Eq. (11).

$$\ln x = [M]\left(k_{\eta 1} + \frac{k_{\eta 3}}{K_{Cl}[Cl^-]}\right)t \quad (10)$$

$$k_{app} = k_{\eta 1} + \frac{k_{\eta 3}}{K_{Cl}[Cl^-]} \quad (11)$$

The rate constant k_{app} was determined by plotting $\ln x$ versus time ($x = ([\mathbf{8}]_{lim} - [\mathbf{8}])/[\mathbf{8}]_{lim} = (D_{lim} - D)/D_{lim}$ with D: absorbance of **8** at t and D_{lim}: final

absorbance of **8**) for different concentrations of Cl^-, added to the cationic complex $\mathbf{2a}^+$ ($C_0 = 0.5$ mM) in DMF just before the addition of morpholine (15 equivalent). Since the nucleophilic attack was considerably slower in the presence of Cl^-, the reactions were performed at 25 °C.

The plot of k_{app} versus the reciprocal of the Cl^- concentration was linear (Fig. 5a). This confirms the mechanism proposed in Scheme 5. $k_{\eta 1}$ was determined from the intercept and $k_{\eta 3}/K_{Cl}$ from the slope.

$$k_{\eta 1} = 0.91\ M^{-1}\ s^{-1} \quad k_{\eta 3}/K_{Cl} = 1.6 \times 10^{-3}\ s^{-1}$$

The value of $k_{\eta 3}$ was determined at 25 °C under stoichiometric conditions (2 equivalent morpholine) and in the absence of chloride ions: $k_{\eta 3} = 94\ M^{-1}\ s^{-1}$ (25 °C). The value of the equilibrium constant K_{Cl} was then calculated: $K_{Cl} = 5.8 \times 10^4\ M^{-1}$ (DMF, 25 °C).

From the values of the equilibrium and rate constants, it comes out that the equilibrium between the cationic complex $\mathbf{2a}^+$ and the neutral complex **3a** lies in favor of **3a** (for $[Cl^-] = 0.5$ mM, then $[\mathbf{3a}]/[\mathbf{2a}^+] = 30$). Since the intercept of the straight line of Fig. 5a differs from zero, it ensues that the neutral complex **3a** reacts in parallel with the cationic complex $\mathbf{2a}^+$ (Scheme 5). The cationic complex $\mathbf{2a}^+$ is intrinsically considerably more reactive than the neutral complex **3a** (by a factor 100). However, in the presence of Cl^-, its concentration may be very low and the neutral complex **3a** may become the main reactive complex. Indeed, if $[Cl^-] = 5 \times 10^{-4}$ M, the contribution of the cationic complex $\mathbf{2a}^+$ (expressed by the value of $k_{\eta 3}/K_{Cl}[Cl^-]$) will be 3.5 times higher than that of the neutral complex **3a** (expressed by the value of $k_{\eta 1}$). But if $[Cl^-] = 5 \times 10^{-3}$ M, the contribution of the cationic complex $\mathbf{2a}^+$ will be only 0.35 of that of the neutral complex **3a** which then plays the essential role in the reaction with morpholine.

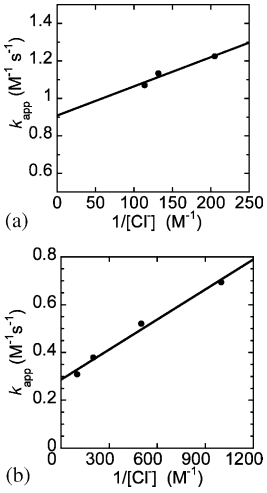

Fig. 5. Kinetics of the reaction of morpholine with the cationic complexes $[(\eta^3\text{-}CH_2\text{–}CH\text{–}CH_2)Pd(PAr_3)_2]^+BF_4^-$ in DMF in the presence of various amount of Cl^- ions added as $n Bu_4NCl$ at 25 °C, monitored by UV spectroscopy. Variation of k_{app} versus the reciprocal of Cl^- concentration (see Eq. (11)). (a) Ar = 4-Cl–C_6H_4 ($\mathbf{2a}^+, BF_4^-$, $C_0 = 0.5$ mM), morpholine (15 equivalent); (b) Ar = 4-Me–C_6H_4 ($\mathbf{2b}^+, BF_4^-$, $C_0 = 1$ mM), morpholine (2 equivalent).

Consequently, depending on the chloride concentration, one may then switch from a nucleophilic attack on the η^3-allyl ligand of the cationic complex to a S_N2' substitution on the η^1-allyl ligand of the neutral complex, which may affect the rate of the reaction and probably the regioselectivity of the reaction. This double effect was observed by Akermark et al. when reacting dimethylamine independently with an isolated cationic complex $[(\eta^3\text{-}CH_3\text{–}CH\text{–}CH\text{–}CH_2)Pd(PPh_3)_2]^+BF_4^-$ and with a neutral complex $\eta^1\text{-}CH_3\text{–}CH{=}CH\text{–}CH_2\text{–}PdCl(PPh_3)_2$, supposedly generated in situ by reaction of $[Pd^{II}(\eta^3\text{-}CH_3\text{–}CH\text{–}CH\text{–}CH_2)(\mu\text{-}Cl)]_2$ with 4 equivalent PPh_3 [8]. However, in this work, neither the equilibrium between the cationic and the neutral complex was considered, nor the effect of the chloride concentration.

Similarly, the rate of the reaction of morpholine (2 equivalent) with the cationic complex $[(\eta^3\text{-}CH_2\text{–}CH\text{–}CH_2)\,Pd\{(4\text{-}Me\text{–}C_6H_4)_3P\}_2]^+BF_4^-$ ($\mathbf{2b}^+, BF_4^-$) ($C_0 = 1$ mM) in DMF decreased upon addition of chloride ions at 25 °C. The equilibrium constant K_{Cl} and the rate constant $k_{\eta 1}$ were determined as for complex $\mathbf{2a}^+, BF_4^-$ (vide supra) in DMF at 25 °C (Fig. 5b, Table 1).

Comparison of that values to those found for the ligand $(4\text{-}Cl\text{–}C_6H_4)_3P$ (Table 1) shows that the formation of the neutral complex η^1-allyl-$PdClL_2$, expressed by the value of K_{Cl}, is less favored than for $(4\text{-}Cl\text{–}C_6H_4)_3P$. This is consistent with the fact that the positive charge on the Pd^{II} is lower when the more electron rich phosphine $(4\text{-}Me\text{–}C_6H_4)_3P$ is considered.

Comparison of the $k_{\eta 3}$ values shows that, as expected, the cationic $[(\eta^3\text{-allyl})Pd(PAr_3)_2]^+$ is less reactive when the electron rich $(4\text{-}Me\text{–}C_6H_4)_3P$ is considered compared to $(4\text{-}Cl\text{–}C_6H_4)_3P$ because the allyl ligand is less electron deficient. Comparison of the $k_{\eta 1}$ values shows that the neutral η^1-allyl-$PdCl(PAr_3)_2$ complex is only slightly less reactive when the electron rich $(4\text{-}Me\text{–}C_6H_4)_3P$ is considered compared to $(4\text{-}Cl\text{–}C_6H_4)_3P$. This is in favor of a S_N2' mechanism with $Pd(PAr_3)_2$ as the leaving group located far from the impact of the nucleophilic attack.

3. Conclusion

The complexes $[Pd(\eta^3\text{-allyl})(\mu\text{-Cl})]_2$ or cationic $[(\eta^3\text{-allyl})PdL_2]^+BF_4^-$ used as precursors in Pd-catalyzed allylic substitutions are not equivalent. Indeed, addition of ligand to the former induces the formation of neutral complexes η^1-allyl-$PdClL_2$ ($L = (4\text{-}Cl\text{–}C_6H_4)_3P$, $(4\text{-}CH_3\text{–}C_6H_4)_3P$, $(4\text{-}CF_3\text{–}C_6H_4)_3P$; L_2 = dppb, dppf) in-

stead of the expected cationic complexes $[(\eta^3\text{-allyl})PdL_2]^+Cl^-$. Those neutral complexes η^1-allyl-$PdClL_2$ are also formed when chloride ions are added to $[(\eta^3\text{-allyl})PdL_2]^+BF_4^-$. The neutral complexes η^1-allyl-$PdClL_2$ are in equilibrium with the cationic complexes $[(\eta^3\text{-allyl})PdL_2]^+$ and Cl^- ($L = (4\text{-}Cl\text{–}C_6H_4)_3P$, $(4\text{-}CH_3\text{–}C_6H_4)_3P$).

The reaction of morpholine with the cationic complexes $[(\eta^3\text{-allyl})Pd(PAr_3)_2]^+BF_4^-$ ($Ar = 4\text{-}Cl\text{–}C_6H_4$, $4\text{-}CH_3\text{–}C_6H_4$) goes slower when performed in the presence of chloride ions. The reaction involves both cationic $[(\eta^3\text{-allyl})Pd(PAr_3)_2]^+$ and neutral η^1-allyl-$PdCl(PAr_3)_2$ complexes, as reactive species. The cationic complex is more reactive than the neutral one. Since the two complexes are involved in equilibrium with the chloride ions, their relative contribution in the reaction strongly depends on the chloride concentration, which controls their relative concentration. At high chloride concentration the neutral η^1-allyl-$PdCl(PAr_3)_2$ becomes the major reactive species.

Consequently, if the catalytic precursor of a Pd-catalyzed allylic substitution is a dimeric complex $[Pd(\eta^3\text{-allyl})(\mu\text{-}Cl)]_2$ associated with monodentate phosphine ligands, in the absence of any chloride ions scavenger, the mechanism of the catalytic reaction may involve the neutral complex η^1-allyl-$PdClL_2$ as the main reactive one and the role of the cationic complex $[(\eta^3\text{-allyl})PdL_2]^+$ may be minimized. This will depend on the initial concentration of $[Pd(\eta^3\text{-allyl})(\mu\text{-}Cl)]_2$ which controls the chloride ions concentration.

Whatever the catalytic precursor, when chloride ions are purposely added in a catalytic allylic substitution, their concentration is high compared to the previous situation. The competition between the cationic and the neutral complexes in their reaction with the nucleophile may then be in favor of the neutral complex η^1-allyl-$PdClL_2$.

In both situations, the rate as well as probably the regioselectivity of the reaction may depend on the chloride concentration, which determines which species, η^1-allyl-$PdClL_2$ or/and $[(\eta^3\text{-allyl})PdL_2]^+$, are involved in the nucleophilic attack. This illustrates the fact that the chloride ions of the catalytic precursors $[Pd(\eta^3\text{-allyl})(\mu\text{-}Cl)]_2$ must not be considered as 'innocent' ligands [27]. Work is in progress to test the effect of chloride ions on the regioselectivity of the reaction in the case of mono- and bidentate ligands.

4. Experimental

General methods. All experiments were performed using standard Schlenk techniques under argon atmosphere. DMF was distilled on CaH_2 and kept under argon. The phosphines PPh_3, $(4\text{-}Z\text{–}C_6H_4)_3P$ ($Z = Cl$, CH_3, CF_3), dppb, dppf (Aldrich and Strem) and the anhydrous n-Bu_4NCl (Aldrich) were commercial. The allyl chloride, cinnamyl chloride, morpholine were commercial (Aldrich) and used after filtration on alumina. $Pd^0\{(4\text{-}Cl\text{–}C_6H_4)_3P\}_4$ [28], $[Pd(\eta^3\text{-}CH_2\text{–}CH\text{–}CH_2)(\mu\text{-}Cl)]_2$ and $[Pd(\eta^3\text{-PhCH–CH–CH}_2)(\mu\text{-}Cl)]_2$ [4,29] were synthesized according to published procedures.

The ^{31}P-NMR spectra were recorded on a Bruker spectrometer (103 MHz) using H_3PO_4 as an external reference, the ^{1}H-NMR spectra on a Bruker spectrometer (250 or 200 MHz). FAB mass spectrometry was performed on a JEOL MS 400 spectrometer. The UV spectra were recorded on a spectrophotometer DU 7400 Beckman. A 1 mm length immersion probe equipped with fiber optics (Hellma) was used for the reactions performed at $-25\,^\circ$C. The conductivity measurements were performed with a conductivity meter (CDM210 Radiometer Analytical) equipped with a cell whose constant k was close to 1 cm^{-1}. Cyclic voltammetry was performed with a homemade potentiostat and a wave form generator GSTP4 (Radiometer Analytical). The current was recorded on an oscilloscope Nicolet 301. The cyclic voltammetry was performed at 0.2 V s^{-1} at a steady gold disk electrode (id 0.5 mm). The counter electrode was a platinum wire (apparent area 0.2 cm^2) and the reference a calomel electrode SCE separated from the cell by a bridge containing 3 ml DMF with n-Bu_4NBF_4, 0.3 M. The cell contained 12 ml of DMF with n-Bu_4NBF_4, 0.3 M.

General procedure for the conductivity measurements. They were performed in a cell thermostated at 25 °C containing 15 ml of DMF. 0.03 mmol of the allyl–Pd^{II} complexes **3a** or **5d** were introduced and the conductivity measured just after introduction and then versus time to monitor the complexes stability.

General procedure for the kinetics of the reaction of morpholine with cationic complexes $[(\eta^3\text{-}CH_2\text{–}CH\text{–}CH_2)PdL_2]^+BF_4^-$ (***2a***$^+$: $L = (4\text{-}Cl\text{–}C_6H_4)_3P$ *and* ***2b***$^+$: $L = (4\text{-}CH_3\text{–}C_6H_4)_3P$) *monitored by UV spectroscopy in the absence and presence of chloride ions*. The reactions were performed in a thermostated cell equipped with a 1 mm length immersion probe. A solution of 25 ml of DMF containing $\mathbf{2a}^+, BF_4^-$ (12 mg, 0.0125 mmol) was transferred under argon to the cell thermostated at $-25\,^\circ$C. The wavelength was selected at 323 nm. After addition of the appropriate amount of morpholine, the increase of the absorbance was recorded versus time until a constant value was reached (Fig. 3a). In other experiments, various amount of n-Bu_4NCl were introduced from a mother solution in DMF, before the addition of morpholine.

4.1. $[\eta^3\text{-}CH_2\text{–}CH\text{–}CH_2)Pd\{(4\text{-}Cl\text{–}C_6H_4)_3P\}_2]^+BF_4^-$ ($\mathbf{2a}^+, BF_4^-$)

It was synthesized according to route A in Scheme 2. A solution of tri(4-chlorophenyl)phosphine (0.366 g, 1 mmol) in acetone (3 ml) was added to a solution of $[Pd(\eta^3\text{-}CH_2\text{–}CH\text{–}CH_2)(\mu\text{-}Cl)]_2$ (0.10 g, 0.27 mmol) in acetone (5 ml), immediately followed by $NaBF_4$ (0.161 g, 1.5 mmol) in water (6 ml). A gray precipitate was formed which was isolated and dried: 0.425 g (81.5% yield). ^{1}H-NMR (200 MHz, $CDCl_3$): δ 3.80 (ddd, 2H, $J_{HH} = 13$, $J_{PH} = 7$, $J_{HH} = 6$ Hz, anti-H), 4.01 (br. d, 2H, $J_{HH} = 7$ Hz, syn-H), 6.02 (tt, 1H, $J_{HH} = 13$, $J_{HH} = 7$ Hz, central H), 7.19–7.32 (m, 24H, aromatic H). ^{31}P-NMR (103 MHz, DMF + acetone-d_6): δ 22.85 (s). MS (FAB+) $C_{39}H_{29}Cl_6P_2Pd^+$: $m/z = 879$ $[M]^+$, 838 $[M - C_3H_5]^+$, 365 $[M - C_3H_5 - 1\ \text{ligand}]^+$.

4.2. $(\eta^1\text{-}CH_2\text{=}CH\text{–}CH_2)PdCl\{(4\text{-}Cl\text{–}C_6H_4)_3P\}_2$ (**3a**)

It was synthesized according to the route B in Scheme 2. A solution of tri(4-chlorophenyl)phosphine (0.64 g, 1.75 mmol) in acetone (5 ml) was added to a solution of $[Pd(\eta^3\text{-}CH_2\text{–}CH\text{–}CH_2)(\mu\text{-}Cl)]_2$ (0.16 g, 0.44 mmol) in acetone (15 ml). After evaporation of the solvent, an orange precipitate was formed which was isolated as a pure compound and dried: 0.62 g (77% yield). ^{1}H-NMR (250 MHz, $CDCl_3$): δ 3.72 (br. d, 4H, $J_{HH} = 10$ Hz, CH_2), 5.61 (quintet, 1H, $J_{HH} = 10$ Hz, central H), 7.35–7.4 (m, 24H, aromatic H). ^{31}P-NMR (103 MHz, $CDCl_3$): δ 21.55 (s). MS (FAB+) $C_{39}H_{29}Cl_7P_2Pd$: $m/z = 879$ $[M - Cl]^+$, 838 $[M - Cl - C_3H_5]^+$.

Complex **3a** was also generated in situ by addition of 1 equiv nBu$_4$NCl (9 μmol) to $\mathbf{2a}^+, BF_4^-$ (9 μmol) in $CDCl_3$ (route C in Scheme 2). The reaction was quantitative. ^{1}H-NMR (250 MHz, $CDCl_3$): δ 3.72 (br. d, 4 H, CH_2), 5.64 (quintet, 1H, $J_{HH} = 10$ Hz, central H), 7.35–7.4 (m, 24H, aromatic H). The ^{1}H-NMR spectrum also exhibits the four sets of protons of the butyl group of nBu$_4$N$^+$.

4.3. $[\eta^3\text{-}CH_2\text{–}CH\text{–}CH_2)Pd\{(4\text{-}CH_3\text{–}C_6H_4)_3P\}_2]^+BF_4^-$ ($\mathbf{2b}^+, BF_4^-$)

The complex was synthesized according to the procedure used for $\mathbf{2a}^+, BF_4^-$ (route A in Scheme 2). The precipitate was crystallized from dichloromethane–petroleum ether. 0.33 g of pale yellow needles was collected (72% yield). ^{1}H-NMR (250 MHz, $CDCl_3$): δ 2.32 (s, 18H, CH_3 ligand), 3.48 (ddd, 2H, $J_{HH} = 13$, $J_{PH} = 7$ Hz, anti-H), 3.95 (br. d, 2H, $J = 6$ Hz, syn-H), 5.93 (tt 1H, $J_{HH} = 13$, $J_{HH} = 6$ Hz, central H), 7.07 (s, 24H, aromatic H). ^{31}P-NMR (103 MHz, acetone-d_6): δ 22.02 (s). MS (FAB+) $C_{45}H_{47}P_2Pd^+$: $m/z = 755$ $[M]^+$, 714 $[M - C_3H_5]^+$.

4.4. $[(\eta^1\text{-}CH_2\text{=}CH\text{–}CH_2)PdCl\{(4\text{-}CH_3\text{–}C_6H_4)_3P\}_2$ (**3b**)

The complex was synthesized from $[Pd(\eta^3\text{-}CH_2\text{–}CH\text{–}CH_2)(\mu\text{-}Cl)]_2$ according to the procedure used for **3a** (route B in Scheme 2). ^{1}H-NMR (200 MHz, $CDCl_3$): δ 2.34 (s, 18H, CH_3 of ligand), 3.72 (m, 4H, CH_2), 5.65 (quintet, 1H, $J_{HH} = 10$ Hz, central H), 7.45 (d, 12H, $J_{HH} = 8$ Hz, aromatic H), 7.62 (d, 12H, $J_{HH} = 8$ Hz, aromatic H). ^{31}P-NMR (103 MHz, $CDCl_3$): δ 21.17 (s). MS (FAB+) $C_{45}H_{47}ClP_2Pd$: $m/z = 755$ $[M - Cl]^+$.

4.5. $[\eta^3\text{-}CH_2\text{–}CH\text{–}CH_2)Pd\{(4\text{-}CF_3\text{–}C_6H_4)_3P\}_2]^+BF_4^-$ ($\mathbf{2c}^+, BF_4^-$)

The complex was synthesized from $[Pd(\eta^3\text{-}CH_2\text{–}CH\text{–}CH_2)(\mu\text{-}Cl)]_2$ (0.05 g, 0.137 mmol) according to the procedure used for $\mathbf{2a}^+, BF_4^-$ (route A in Scheme 2). The precipitate was crystallized from dichloromethane. 0.23 g of white crystals was collected (72% yield). ^{1}H-NMR (250 MHz, acetone-d_6): δ 3.84 (ddd, 2H, $J_{HH} = 12$, $J_{PH} = 7$ Hz, anti-H), 4.32 (br. d, 2H, $J_{HH} = 7$ Hz, syn-H), 6.26 (tt, 1H, $J_{HH} = 12$, $J_{HH} = 7$ Hz, central H), 7.62 (s, 24H, aromatic H). ^{31}P-NMR (103 MHz, acetone-d_6): δ 24.04 (s).

4.6. $[(\eta^1\text{-}CH_2\text{=}CH\text{–}CH_2)PdCl\{(4\text{-}CF_3\text{–}C_6H_4)_3P\}_2$ (**3c**)

The complex was synthesized from $[Pd(\eta^3\text{-}CH_2\text{–}CH\text{–}CH_2)(\mu\text{-}Cl)]_2$ (0.05 g, 0.137 mmol) according to the procedure used for **3a** (route B in Scheme 2). 0.18 g of crystals was collected (59% yield). ^{1}H-NMR (250 MHz, acetone-d_6): δ 3.61 (d, 4H, $J_{HH} = 10$ Hz, CH_2), 5.70 (quintet, 1H, $J_{HH} = 10$ Hz, central H), 7.61 (s, 24H, aromatic H). ^{31}P-NMR (103 MHz, acetone-d_6): δ 23.33 (s).

4.7. $[\eta^3\text{-}Ph\text{–}CH\text{–}CH\text{–}CH_2)Pd\{(4\text{-}Cl\text{–}C_6H_4)_3P\}_2]^+BF_4^-$ ($\mathbf{2a'}^+, BF_4^-$)

The complex was synthesized from $[Pd(\eta^3\text{-}Ph\text{–}CH\text{–}CH\text{–}CH_2)(\mu\text{-}Cl)]_2$ according to the procedure used for $\mathbf{2a}^+, BF_4^-$ (route A in Scheme 2). Pale yellow crystals (61% yield). ^{1}H-NMR (250 MHz, $CDCl_3$): δ 3.67 (dd, 1H, $J_{HH} = 7$, $J_{PH} = 7$ Hz, syn-H of CH_2), 3.72 (dd, 1H, $J_{HH} = 11$, $J_{PH} = 11$ Hz, anti-H of CH_2), 5.69 (dd, 1H, $J_{HH} = 10$, $J_{PH} = 10$ Hz, PhCH-anti), 6.34 (ddd, 1H, $J_{HH} = 11$, $J_{HH} = 10$, $J_{HH} = 7$ Hz, central H), 6.8–7.0 (m, 5H, H of Ph), 7.1–7.4 (m, 24H, aromatic H of ligand). ^{31}P-NMR (103 MHz, $CDCl_3$): δ 22.95 (d, 1P, $J_{PP} = 45$ Hz), 24.62 (d, 1P, $J_{PP} = 45$ Hz). MS (FAB+) $C_{45}H_{33}Cl_6P_2Pd^+$: $m/z = 955$ $[M]^+$, 838 $[M - PhC_3H_4]^+$.

4.8. (η^1-Ph–CH=CH–CH_2)PdCl{(4-Cl–C_6H_4)$_3$P}$_2$ (**3a′**)

It was synthesized from [Pd(η^3-Ph–CH–CH–CH_2)(μ-Cl)]$_2$ according to route B in Scheme 2 or by addition of 1 equiv nBu$_4$NCl to **2a′**$^+$, BF_4^- in chloroform (route C in Scheme 2). ^{1}H-NMR (250 MHz, $CDCl_3$): δ 3.15 (d, 2H, $J_{HH} = 9$ Hz), 5.28 (d, 1H, $J_{HH} = 13$ Hz), 6.06 (dd, 1H, $J_{HH} = 13$, $J_{HH} = 9$ Hz, central H), 7.26–7.61 (m, 29H, H of Ph and aromatic H of ligand). ^{31}P-NMR (103 MHz, $CDCl_3$): δ 21.89 (s). MS (FAB+) $C_{45}H_{33}Cl_7P_2Pd$: $m/z = 955$ [M − Cl]$^+$, 838 [M − Cl-PhC_3H_4]$^+$.

4.9. (η^1-CH_2=CH–CH_2)PdCl(dppb) (**5d**)

It was synthesized according to route B in Scheme 3: dppb (0.114 g, 0.27 mmol) in acetone (5 ml) was added to a solution of [Pd(η^3-CH_2–CH–CH_2)(μ-Cl)]$_2$ (0.05 g, 0.136 mmol) in acetone (2.5 ml). After half an hour, the solvent was concentrated. A pale yellow precipitate appeared. After filtration, the solid was dissolved in dichloromethane and crystallized in petroleum ether. 0.115 g was collected (70% yield). ^{1}H-NMR (250 MHz, $CDCl_3$): δ 1.91 (br. s, 4H, CH_2 of dppb), 2.83 (br. s, 4H, CH_2 of dppb), 3.75 (br. m, 4H, CH_2), 5.63 (quintet, 1H, $J_{HH} = 10$ Hz, central H of CH_2=CH–CH_2), 7.43 (br. s, 12 H, aromatic H), 7.55 (br. s, 8 H, aromatic H). ^{1}H-NMR (250 MHz, DMF-d_7): δ 1.18 (br. s, 4 H, CH_2 of dppb), 2.96 (br. s, 4H, CH_2 of dppb), 3.75 (br. m, 4H, CH_2), 5.98 (quintet, 1H, $J_{HH} = 10.5$ Hz, central H of CH_2=CH–CH_2), 7.54 (br. s, 12H, aromatic H), 7.69 (br. s, 8H, aromatic H). ^{31}P-NMR (103 MHz, $CDCl_3$): δ 18.47 (s). FAB+ MS $C_{31}H_{33}P_2PdCl$: $m/z = 573$ [M − Cl]$^+$, 532 [M − Cl − C_3H_5]$^+$.

4.10. (η^1-CH_2=CH–CH_2)PdCl(dppf) (**5e**)

It was synthesized according to the procedure used for **5d**. Orange crystals (52% yield). ^{1}H-NMR (250 MHz, $CDCl_3$): δ 3.99 (br. m, 4H, =CH_2), 4.43 (m, 10H, H of Cp), 5.95 (quintet, 1H, $J_{HH} = 10.5$ Hz, central H of CH_2=CH–CH_2), 7.48 (m, 12H, aromatic H), 7.60 (m, 8H, aromatic H). ^{31}P-NMR (103 MHz, $CDCl_3$): δ 22.96 (s). (FAB+) $C_{37}H_{33}ClFeP_2PdCl$: $m/z = 701$ [M − Cl]$^+$, 660 [M − Cl − C_3H_5]$^+$.

Acknowledgements

This work has been supported by the Centre National de la Recherche Scientifique (CNRS-ENS-UPMC, UMR 8640) and the Ministère de la Recherche (Ecole Normale Supérieure). We thank Johnson Matthey for a generous loan of sodium tetrachloropalladate.

References

[1] (a) J. Tsuji, Palladium Reagents and Catalysts, John Wiley & Sons, Chichester, 1996, p. 290;
(b) S.A. Godleski, in: B.M. Trost, I. Flemming (Eds.), Comprehensive Organic Synthesis, vol. 4, Pergamon, Oxford, 1991;
(c) C.G. Frost, J. Howard, J.M.J. Williams, Tetrahedron: Asymmetry 3 (1992) 1089;
(d) G. Consiglio, R. Waymouth, Chem. Rev. 89 (1989) 257;
(e) A. Pfaltz, Acc. Chem. Rev. 26 (1993) 339–345;
(f) T. Hayashi, in: I. Ojima (Ed.), Catalytic Asymmetric Synthesis, VCH, New York, 1993, p. 325;
(g) B.M. Trost, D.L. Van Vranken, Chem. Rev. 96 (1996) 395;
(h) B.M. Trost, Acc. Chem. Res. 29 (1996) 355;
(i) E.I. Negishi, Handbook of Organopalladium Chemistry for Organic Synthesis, 2002, vol. 2, Wiley Interscience, New York, pp. 1663–2027.
[2] (a) C. Amatore, A. Jutand, G. Meyer, L. Mottier, Chem. Eur. J. 5 (1999) 466;
(b) C. Amatore, S. Gamez, A. Jutand, Chem. Eur. J. 7 (2001) 1273;
(c) C. Amatore, S. Gamez, A. Jutand, G. Meyer, L. Mottier, Electrochim. Acta 46 (2001) 3237.
[3] C. Amatore, A. Jutand, M.A. M'Barki, G. Meyer, L. Mottier, Eur. J. Inorg. Chem. (2001) 873.
[4] J. Powell, B.L. Shaw, J. Chem. Soc. A (1967) 1839.
[5] P. Braunstein, F. Naud, A. Dedieu, M.-M. Rohmer, A. DeCian, S.J. Rettig, Organometallics 20 (2001) 2966.
[6] M. Kollmar, G. Helmchen, Organometallics 21 (2002) 4771.
[7] G. Malaisé, L. Barloy, J.A. Osborn, N. Kyritsakas, C. R. Chimie 5 (2002) 289.
[8] B. Akermark, G. Akermark, L.S. Hegedus, K. Zetterberg, J. Am. Chem. Soc. 103 (1981) 2037.
[9] (a) J.E. Bäckvall, R.E. Nordberg, J. Am. Chem. Soc. 103 (1981) 4959;
(b) R.E. Nordberg, J.E. Bäckvall, J. Organomet. Chem. 285 (1985) C24.
[10] M. Kawatsura, Y. Uozumi, T.J. Hayashi, Chem. Soc. Chem. Commun. (1998) 217.
[11] (a) G.C. Lloyd-Jones, S.C. Stephen, J. Chem. Soc. Chem. Commun. (1998) 2321;
(b) G.C. Lloyd-Jones, S.C. Stephen, Chem. Eur. J. 4 (1998) 2539.
[12] B.M. Trost, F.D. Toste, J. Am. Chem. Soc. 121 (1999) 4545.
[13] A mixed neutral complex (η^3-CH_2–CH–CH_2)PdCl(PPh_3) **4** was generated only by addition of two equiv. PPh_3 to the dimer [Pd(η^3-CH_2=CH–CH_2)(μ-Cl)]$_2$ (Route F of Scheme 2) [3,4]. Attempt to synthesize such a complex with (4-CF_3–C_6H_4)$_3$P led to a complex mixture.
[14] In a previous work [3], we established that the phosphonium salt was formed from the neutral complex η^1-RCH=CH–CH_2–PdCl(PPh_3)$_2$ by a reversible reductive elimination which also generated a Pd^0 complex. This reaction became preponderant in the presence of any chemical able to stabilize or to react with the Pd^0 complex (dba, extra PPh_3, dioxygen) [3].
[15] For a review on the characterization of cationic Pd^{II} complexes by conductivity measurements in DMF, see: A. Jutand, Eur. J. Inorg. Chem. (2003) 2017.
[16] This value was calculated at 25 °C by addition of the conductivity of **2a**$^+$, BF_4^-, 2 mM in DMF (69 μs cm^{-1}) determined above (see text) to that of nBu$_4$NCl, 2 mM in DMF (131 μs cm^{-1}) [17] and subtraction of the conductivity of nBu$_4$NBF_4, 2 mM in DMF (136 μs cm^{-1}) [2a].
[17] A. Jutand, A. Mosleh, Organometallics 14 (1995) 1810.
[18] The conductivity slightly increased to 20 μs cm^{-1}. This might be due to the formation of a small amount of an allyl-phosphonium salt [14].

[19] This value has been calculated at 25 °C from the known conductivity of $[(\eta^3\text{-}CH_2\text{–}CH\text{–}CH_2)Pd(dppb)]^+AcO^-$ 2 mM in DMF (82 μs cm^{-1}) [2b] by addition of the conductivity of nBu$_4$NCl, 2 mM in DMF (131 μs cm^{-1}) [17] and subtraction of the conductivity of nBu$_4$NOAc, 2 mM in DMF (89 μs cm^{-1}) [2a].
[20] (a) J. Powell, B.L. Shaw, J. Chem. Soc. A (1968) 774;
(b) T. Hayashi, A. Yamamoto, T. Hagihara, J. Org. Chem. 51 (1986) 723.
[21] M. Baboulène, J.L. Torregrosa, V. Spéziale, A. Lattes, Bull. Soc. Chim. Fr. 11–12 (1980) 565.
[22] The kinetics was monitored at −25 °C. Monitoring the kinetics by cyclic voltammetry at such a low temperature was thus a problem due to the high resistivity of the solution.
[23] O. Kuhn, H. Mayr, Angew. Chem. Int. Ed. 38 (1999) 343.
[24] In that case the complex exhibited an absorption band at 314 nm which disappeared upon addition of morpholine. Two new absorption bands appeared at 296 and 356 nm. The kinetics was monitored by recording the increase of the absorbance of the Pd^0 at 296 nm.
[25] Since the reaction was performed under stoichiometric conditions, according to the mechanism of Scheme 4, the kinetic law is then $1/x = k_{\eta 3}C_0(2+k_{\eta 3}/k_2)t+1$ if k_2 is the rate constant of the second step (deprotonation). If $k_2 \gg k_{\eta 3}$, the rate law is then $1/x = 2k_{\eta 3}C_0t+1$.
[26] For S_N2' substitution of morpholine on allyl bromide see: G. Butler, R.L. Bunch, J. Am. Chem. Soc. 71 (1949) 3120.
[27] For a review on the halide effects in transition metal catalysis, see: K. Fagnou, M. Lautens, Angew. Chem. Int. Ed. 41 (2002) 26.
[28] Y. Takahashi, Ts. Ito, S. Sakai, Y. Ishii, J. Chem. Soc. Chem. Commun. (1970) 1065.
[29] P.M. Auburn, P.B. Mackenzie, B. Bosnish, J. Am. Chem. Soc. 107 (1985) 2033.